

## Computational fluid dynamic study of upper airway flow to predict the success of oral appliances in treating sleep apnea

Moyin Zhao<sup>1</sup>, Tracie Barber<sup>1</sup>, Peter Cistulli<sup>2,3,4</sup>, Kate Sutherland<sup>3,4</sup>, Gary Rosengarten<sup>1</sup>

<sup>1</sup>School of Mechanical Engineering,  
University of New South Wales, Sydney, New South Wales 2032, Australia

<sup>2</sup>Sydney Medical School,  
The University of Sydney, Sydney, New South Wales 2006, Australia

<sup>3</sup>Centre for Sleep Health & Research,  
Royal North Shore Hospital, St Leonards, New South Wales 2065, Australia

<sup>4</sup>Sleep & Circadian Group,  
Woolcock Institute of Medical Research, Glebe, New South Wales 2037, Australia

### Abstract

In this study we used computational fluid dynamics (CFD) to analyse the therapeutic effect of an oral device (mandibular advancement splint – MAS) that protrudes the lower jaw during sleep on obstructive sleep apnea (OSA). Clinical data of 4 patients were used for CFD analysis, with patient selection being on the basis of their known different treatment responses. Anatomically accurate upper airway (UA) computational models were reconstructed from magnetic resonance images (MRI) with and without a MAS device fitted. CFD simulations of airflow were performed at the maximum flow rate during inspiration. Factors such as velocity, pressure, area in the restricted region is closely associated with the change in severity of OSA for patients using MAS. The CFD analysis clearly demonstrated the way MAS treatment affected the patients' UA airflow patterns. The results show that there is a strong relationship between the calculated flow and physical properties and the treatment response. We plan to study more patients in order to develop a model to predict treatment response of MAS by patient-specific CFD results.

**Keywords:** OSA, upper airway, MAS, MRI, CFD, pressure drop

### Introduction

Obstructive sleep apnea (OSA) syndrome is a common sleep-disorder of both adults and children, which is characterized by repetitive episodes of complete (apnea) or partial (hypopnea) collapse of the airway during sleep [10], resulting in sleep disturbance and oxygen desaturation. A range of daytime symptoms, such as sleepiness, memory and concentration deficits, are often evident. The severity of OSA is defined by the Apnea and Hypopnea Index (AHI), derived from the total number of apnoeas and hypopnoeas per hour of sleep [4].

Mandibular Advancement Splints (MAS) offer one approach to decrease the AHI, using a custom-made mouthguard worn during sleep to protrude the lower jaw (mandible). This movement has been shown to increase pharyngeal area, especially in the lateral dimension, thereby reducing the collapsibility of the airway during sleep [6].

Despite the high acceptance among patients, MAS treatment has been criticised for its suboptimal cure rate (approx 50% [1]) and varying response among patients. Generally, a lower success rate is found in severe OSA patient compared with mild to moderate

cases (defined by AHI) [4]. The individual treatment outcome remains an elusive goal due to incomplete understanding of the mechanisms of action in the MAS treatment [3].

Recently, computational fluid dynamics (CFD) has been introduced as a method for modelling the UA flow field. Martonen et al. [9] investigated the laminar flow in a teaching UA model. The transitional flow pattern in UA was indicated by Heenan et al. [7] in 2003. They applied the Reynolds averaged Navier–Stokes (RAN) equations on a geometry-idealized UA model. In 2006, Xu et al. [12] performed their CFD analysis on CT based anatomical-accurate UA geometry of children. Later, Collins et al. [2] compared the CFD result of idealized and patient-specific UA model, which indicated that a more accurate flow pattern can be found in realistic UA models. Recently in 2009, Mylavarapu et al. [10] used different turbulent models on an anatomical-accurate UA model. The K- $\omega$  model was shown to be the best match to experimental results based with a limited grid density.

In this research, we established upper airway models of four OSA patients for use in CFD. They were selected on the basis of their varied treatment response to MAS. In the CFD analysis, the flow in each section of upper airway are calculated and compared.

### Materials

Patient	Gender	Age	BMI	AHI (WO)	AHI (W)
R	Male	52	29.41	41.5	2.1
P-R	Male	31	24.26	28.4	13.9
N-R	Male	49	36.65	29.2	23.6
F	Male	57	28.34	16.0	31.7

Table 1 General characteristics of 4 patients. (R = Responder, P-R = Partial-responder, N-R = Non-responder, F = Failure, WO = without MAS, W = with MAS)

### Numerical modelling

#### Medical imaging

For this study, we chose 4 patients with different levels of improvement in their AHI after MAS treatment. They represent 4 different types of treatment outcome defined as Complete-responder (post-treatment AHI<5/hr), Partial-responder ( $\geq 50\%$  reduction in AHI), Non-responder (<50% AHI reduction) and Failure (increase post-treatment AHI). Details of patients' data can be found in Table 1. The custom-made 2-piece MAS that patients use was fabricated by SomnoDentMAS; SomnoMed Ltd, Crows Nest, Australia.

**Geometric modelling**

The 3-D upper airway computational models of these four patients are generated from Magnetic Resonance image (MRI). Two sagittal scans (with and without MAS) were performed for each patient when awake by using of a Philips INTERA 1.5T scanner (Philip Electronics, Netherlands). Patients are required to lie in supine position. 50 slices (512 x 512 matrix) are taken from the level above nasopharynx to the level below vocal cord with a thickness of 3mm. The pixel spacing is 0.488mm x 0.488mm. During scanning, the regular breathing and swallowing were permitted.

The MRI data (DICOM image) were processed in Amira 5 (Visage Imaging, United States). We defined the geometry of the upper airway model from the horizontal cross-section of hard palate down to vocal cords (Figure 1). These label fields were created for indentifying the UA on each slice, using a threshold from 0 to 180. The wall of airway was created from these masks as a surface model in Amira 5.2.2 and exported into ANSYS ICEM CFD 12.1(ANSYS, United States) for mesh generation. Finally, the surface was refined using a vertex-averaging smoothing algorithm.

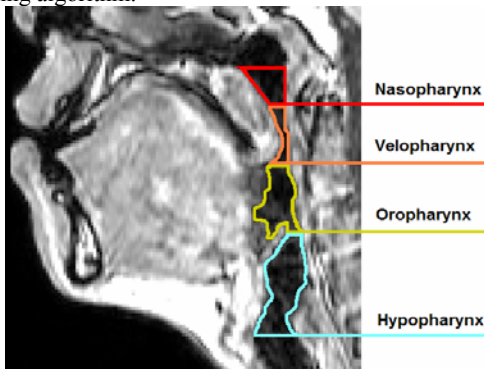


Figure 1 Anatomy of human upper airway

**Meshing**

An unstructured tetrahedral volume mesh was generated with 5 inflation layers attached to the wall boundary. In order to reduce computational expense while maintaining the accuracy, a hybrid mesh method was used. We allowed structured hexahedra grids exist at the core of the unstructured tetrahedral mesh (Figure 2). A mesh convergence test was performed on models of different grid number. Figure 3 gives us a clear view of the velocity data on a line along the UA model. The 1.3 million-mesh size was selected for modelling because it had an acceptable accuracy and saved 20%-30% computational time compared to the model that had 1.6 million and 1.8 million grid points. The maximum grid edge length was 0.5 mm.

**Turbulence modelling**

We performed the simulations using the ANSYS CFX 12.1 (ANSYS, United States). Considering the low Mach number air flow, the flow was modelled as incompressible. The Reynolds number (Re) of the flow in the upper airway was determined by:

$$Re = \frac{QD}{\nu A} \tag{1}$$

$$D = \frac{4A}{P} \tag{2}$$

Q: volumetric flow rate, D: hydraulic diameter of UA, A: cross-sectional area of UA, P: perimeter of the airway of UA,  $\nu$ : Kinematic viscosity.

The Re was varied from 426 to 2834 in the UA model which means the flow in either laminar or transitional. The highest Re located in velopharynx, which had the smallest cross-sectional area. Reynolds-averaged K- $\omega$  model was selected as the turbulence model [10]. High resolution was chosen as the

advection scheme. The results was considered as converged when the residual level dropped by the defined residual target of  $10^{-6}$ .

**Boundary conditions**

The inlet boundary was defined at the nasopharynx, while outlet boundary was set of the vocal cord (Figure 1). A maximum inlet volume flow rate 166ml/s (10L / min) was used in the simulation, which equals 0.0002 kg/s for air at 25 °C [5]. The turbulence intensity was set as 10% [10]. An average static pressure of -267 Pascal (relative to 1 atm) was used at the outlet [11]. The wall of whole upper airway was assumed as no-slip and smooth. The simulations were run on a Q9550 desktop PC with 16 GB Ram for roughly 6 hours.

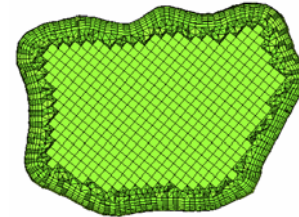


Figure 2 The hybrid mesh in ICEM. This is a cut plane in geometry.

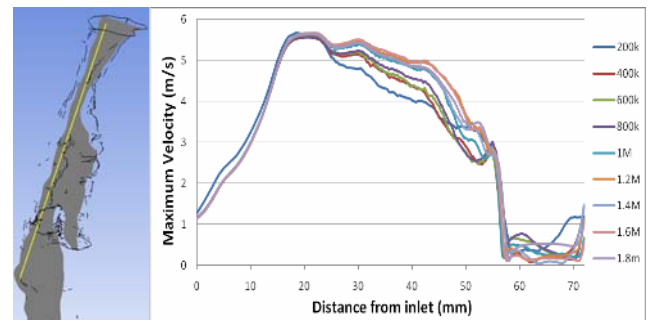


Figure 3 Plot of axial velocity contours along the line shown in the image on the left.

**Results**

**Geometry overview**

Model	AHI	Volume (m <sup>3</sup> )	Restricted area (m <sup>2</sup> )	Lateral (m)	Antero-posterior (m)	
R	WO	41.5	1.25x10 <sup>-5</sup>	2.04x10 <sup>-5</sup>	0.0073	0.0026
	W	2.1	1.63x10 <sup>-5</sup>	3.30x10 <sup>-5</sup>	0.01	0.0034
P-R	WO	28	1.79x10 <sup>-5</sup>	1.78x10 <sup>-5</sup>	0.0081	0.0021
	W	14	2.22x10 <sup>-5</sup>	2.52x10 <sup>-5</sup>	0.0095	0.0023
N-R	WO	29	2.65x10 <sup>-5</sup>	2.49x10 <sup>-5</sup>	0.0069	0.0052
	W	23	1.65x10 <sup>-5</sup>	3.71x10 <sup>-5</sup>	0.0183	0
F	WO	28	1.17x10 <sup>-5</sup>	2.97x10 <sup>-5</sup>	0.0099	0.003
	W	14	1.01x10 <sup>-5</sup>	1.81x10 <sup>-5</sup>	0.0083	0.0015

Table 2 The summary of geometrical parameters for all UA models. (R = Responder, P-R = Partial-responder, N-R = Non-responder, F = Failure, WO = without MAS, W = with MAS, Lateral = the width between the left side and right side of airway, Antero-posterior = the distance between the front and back of airway)

From geometric dimension of the upper airway among 4 patients, an increase in airway volume could be found in Responder and Partial-responder, which were 30.4% and 23.9% respectively. There was a dramatic 37.7% decrease in the airway volume of Non-responder. In the Failure case, there was a small reduction of 13.7% in volume can be found.

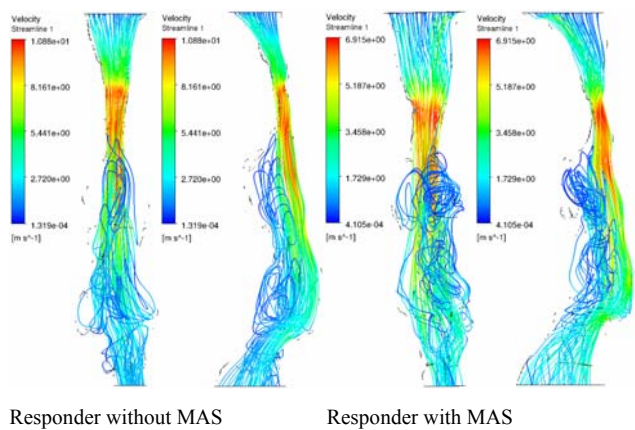
As the enormous restriction in cross-sectional area, the velopharynx was considered as the most critical region along the whole upper airway structure in terms of collapsibility [8]. After

using MAS, this restricted region enlarged for all cases except the Failure. The Responder had the highest increase which was 61.7% in this area followed by the Non-responder (49.0%) and Partial-responder (41.8%). There was a 39.0% decrease in the velopharynx area of the Failure.

The result showed that an increase in minimum cross-sectional area could generally lead to the reduction in AHI. In the Non-responder case, nevertheless, the AHI reduction was too small and a 49% gain in restricted area was found after using MAS.

An investigation at the anteroposterior (depth) and lateral dimension (width) of this cross-section might help us understand more. In the Responder geometries, a 37.0% increase could be found in width and 30.8% also be found in depth. The increase of the width was 17.3% lower in the Partial-responder, and the growth of depth was only 9.5%. What drew our attention was the dramatic 165.2% enlargement in width of the critical area in Non-responder, while, the depth came to zero due to the soft palate attached the posterior wall of the airway. In the Failure case, the width and the depth were shortened by 16% and 50% respectively. The results indicate that the MAS could change more in lateral width of airway than anteroposterior depth. However, the depth might play a more important role in alleviating OSA syndrome.

**Velocity streamlines of four patients**



Responder without MAS

Responder with MAS

Figure 4 Velocity Streamline profiles (m/s) as the results of simulation in CFX. The colour scales are different in each plot.

The streamline plot provided a straight view of flow motion inside upper airway models (Figure 4). The results indicated a similar flow pattern for almost all the models. The air flow was restricted around uvula (the end of soft palate). It then attaches to the posterior wall of velopharynx and oropharynx before travelling through the vocal cord, which is named as the ‘‘Pharynx Jet’’ [7]. Recirculation flows will be generated in oral cavity and the space between the root of tongue and epiglottis. The only exceptional flow pattern can be found in the model of Failure without MAS. The abnormal swelling at the posterior pharyngeal wall forces the airflow going into oral cavity, while creating eddies around the back wall of oropharynx. The airflow changes direction again at epiglottis. The opening epiglottis can also restrict the flow slightly in models of Partial responder and Failure. Moreover, the asymmetric velopharyngeal structure in models like Partial-responder with and without MAS, the Failure with MAS can result in a sideways motion of airflow in oropharynx. That will induce a recirculation region occurring at the other side of oropharynx.

**The Maximum velocity and Minimum pressure**

In each model, horizontal cross-sectional planes are created in every 5 mm along the airway structure (Figure 5). The planes are dependent on the length of airway. In Figure 5, the magnitude of

the maximum velocity and minimum pressure in each plane is plotted versus the distance from inlet boundary. The MAS treatment response is then clearly demonstrated. The plot of the Responder indicates that a successful treatment can result in a significant reduction in velocity rise and pressure drop at around 3 mm, which is the restricted area position in velopharynx. A reduction in the effectiveness of MAS can be found in the Partial responder and Non-responder based on these figures. A significant velocity rise and pressure drop increase occurs in the Failure. In all, these velocity and pressure results demonstrate a strong relationship with the treatment results.

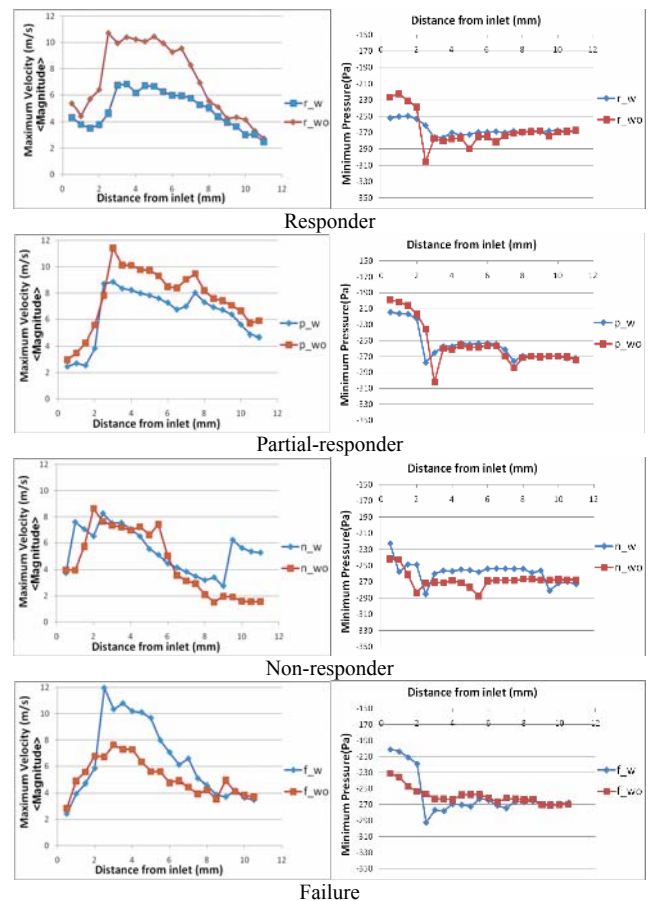
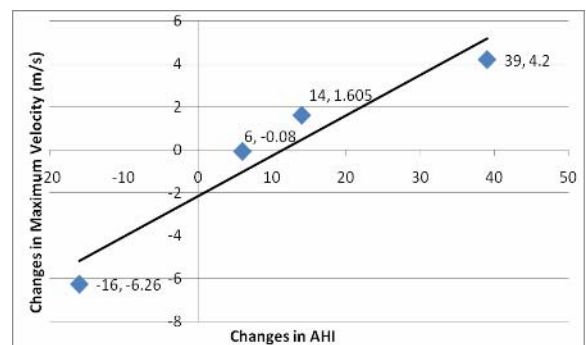


Figure 5 The maximum magnitude of the velocity (m/s) and minimum pressure (Pa) value along each UA model (WO = without MAS, W = with MAS).

Figure 6 depicts the changes in velocity and relevant pressure versus patients’ AHI data. With more patients’ data, this plot will provide more insight.



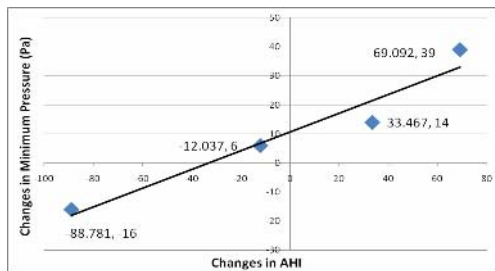


Figure 6 Relationship between velocity magnitude and minimum pressure values with AHI changes. The black solid lines are the linear trendlines of data.

## Conclusion

This paper successfully shows the usefulness of applying CFD to determine the different responses of MAS treatment on OSA patients. The restricted area at velopharynx directly induced a jet flow with significant velocity increase and pressure drop. The flow separated in oropharynx. A circulation zone occurred in the oral cavity, while the main air flow was remained attached at the posterior wall of the airway. As a result, there was a strong relationship between flow parameters and patients' AHI data. In this study, only one case was picked from each patient's group. For statistical significance we will be using a full data set to complete the predictive model which hopefully can be utilised in future clinical treatment.

## References

- [1] Cistulli, P. A., H. Gotsopoulos, et al. (2004). "Treatment of snoring and obstructive sleep apnea with mandibular repositioning appliances." *Sleep Medicine Reviews* 8(6): 443-457.
- [2] Collins, T.-P., G.-R. Tabor, P.-G. Young. (2007). "A Computational Fluid Dynamics Study of Inspiratory Flow in Orotracheal Geometries." *Medical and Biological Engineering and Computing* 45: 829-836.
- [3] De Backer, J. W., O. M. Vanderveken, et al. (2007). "Functional imaging using computational fluid dynamics to predict treatment success of mandibular advancement devices in sleep-disordered breathing." *Journal of Biomechanics* 40(16): 3708-3714.
- [4] Ferguson K.-A., R. Cartwright, R. Rogers, et al. (2006) "Oral appliances for snoring and obstructive sleep apnea: a review." *Sleep* 29:244–262.
- [5] Franz, C., A.-V. Hirtum, P.-Y. Lagr'ee, et al. (2006). "Simulation of the Retroglossal Fluid-Structure Interaction During Obstructive Sleep Apnea." *Lecture Notes in Computer Science* (2006) volume 4072, pp. 48–57.
- [6] Gotsopoulos, H., C. Chen, J. Qian. (2002) "Oral appliance therapy improves symptoms in obstructive sleep apnea: a randomized, controlled trial." *Am J Respir Crit Care Med* 166:743–748.
- [7] Heenan, A.-F., E. Matida, A. Pollard, et al. (2003)"Experimental Measurements and Computational Modeling of the Flow Field in an Idealized Human Oropharynx." *Journal of Experiments in Fluids* 35(2003) 70-84.
- [8] Jeong, S.-J., W.-S. Kim, et al. (2007). "Numerical investigation on the flow characteristics and aerodynamic force of the upper airway of patient with obstructive sleep apnea using computational fluid dynamics." *Medical Engineering & Physics* 29(6): 637-651.
- [9] Martonen, T.B.,L. Quan, Z. Zhang, et al (2002). "Flow simulation in the human upper respiratory tract," *Cell Biochem. Biophys.* 37, 27.
- [10] Mylavarapu, G., S. Murugappan, et al. (2009). "Validation of computational fluid dynamics methodology used for human upper airway flow simulations." *Journal of Biomechanics* 42(10): 1553-1559.
- [11] Tortora, G. J. and B. Derrickson (2006). *Introduction to the human body - the essentials of anatomy and physiology*. New York, Wiley.
- [12] Xu, C., S. Sin, et al. (2006). "Computational fluid dynamics modeling of the upper airway of children with obstructive sleep apnea syndrome in steady flow." *Journal of Biomechanics* 39(11): 2043-2054.